Heat and Technology
Vol. 32, n. 1-2, 2014

MAGNETIC FIELD EFFECT ON NATURAL CONVECTION IN A NANOFLUID-FILLED ENCLOSURE WITH NON-UNIFORM HEATING ON BOTH SIDE WALLS

Imen Mejri[1], Ahmed Mahmoudi[1], Mohamed Ammar Abbassi[1] and Ahmed Omri[1]

[1] UR:Unité de Recherche Matériaux, Energie et Energies Renouvelables (MEER), Faculté des Sciences de Gafsa, B.P.19, Zarroug, Gafsa, 2112, Tunisie

ABSTRACT

This paper examines the natural convection in a square enclosure filled with a water-Al_2O_3 nanofluid and is subjected to a magnetic field. The side walls of the cavity have spatially varying sinusoidal temperature distributions. The horizontal walls are adiabatic. Lattice Boltzmann method (LBM) is applied to solve the coupled equations of flow and temperature fields. This study has been carried out for the pertinent parameters in the following ranges: Rayleigh number of the base fluid, Ra=10^3 to 10^5, Hartmann number varied from Ha=0 to 50, phase deviation (γ=0, $\pi/4$, $\pi/2$, $3\pi/4$ and π) and the solid volume fraction of the nanoparticles between $\phi = 0$ and 6%. The results show that the heat transfer rate increases with an increase of the Rayleigh number but it decreases with an increase of the Hartmann number. Also it is observed that the Phase deviation control the heat transfer rate.

1. Introduction

The problem of natural convection in square enclosures has many engineering applications such as: cooling systems of electronic components, building and thermal insulation systems, built-in-storage solar collectors, nuclear reactor systems, food storage industry and geophysical fluid mechanics [1]. Some practical cases such as the crystal growth in fluids, metal casting, fusion reactors and geothermal energy extractions, natural convection is under the influence of a magnetic field [2-3]. Badawi et al. [4] studied numerically MHD natural convection iso-flux problem inside a porous media filled inclined rectangular enclosures. The results show that both the magnetic force and the inclination angle have significant effect on the flow field and iso- heat flux in porous medium. Abishek et al. [5] studied numerically natural convection of an electrically conducting fluid due to both heat and solutal transfer, in a square enclosure filled with porous medium, subjected to a uniform magnetic field applied parallel to the adiabatic walls on the plane of the enclosure. It is found that the effect of the applied magnetic field is significant to the extent that convection is completely suppressed for large values of Ha. Ahmed et al.[6] investigated the free convective oscillatory flow of a viscous incompressible and electrically conducting fluid past a vertical porous plate in sleep flow regime with variable suction and periodic plate temperature in presence of a uniform transverse magnetic field. Shehadeh et al. [7] investigated the magneto hydrodynamics natural convection heat transfer with Joule and viscous heating effects inside a porous media filled inclined rectangular enclosures; it is found that the Gebhart number has the largest effect on heat transfer and fluid flow. Lai and Yang [8] performed mathematical modeling to simulate natural convection of Al_2O_3/water nanofluids in a vertical square enclosure using the Lattice Boltzmann method. The results indicated that the average Nusselt number increased with the increase of Rayleigh number and particle volume concentration. The average Nusselt number with the use of nanofluid was higher than the use of water under the same Rayleigh number. Mahmoudi et al. [9] presented a numerical study of natural convection cooling of two heat sources vertically attached to horizontal walls of a cavity. The results indicated that the flow field and temperature distributions inside the cavity were strongly dependent on the Rayleigh numbers and the position of the heat sources. The results also indicated that the Nusselt number was an increasing function of the Rayleigh number, the distance between two heat sources, and distance from the wall and the average Nusselt number increased linearly with the increase in the solid volume fraction of nanoparticles

The LBM is an applicable method for simulating fluid flow and heat transfer [10–11]. This method was also applied to simulate the MHD [12] and, recently, nanofluid [13] successfully. The aim of the present study is to identify the ability of Lattice Boltzmann Method (LBM) for solving nanofluid, magnetic field simultaneously in the presence of a linear boundary condition. Moreover, the effect of magnetic field and its direction on the heat transfer in the cavity. In fact, it is endeavored to express the best situation for heat transfer and fluid flow with the considered parameters. Hence, the Al_2O_3–water nanofluid on laminar natural convection heat transfer at the presence of a magnetic field in linear temperature distribution on vertical side walls of the cavity by LBM was investigated. The aim of the present study is to identify the ability of Lattice Boltzmann Method (LBM) for solving nanofluid, magnetic field simultaneously in the presence of a sinusoidal boundary condition. Moreover, the effects of magnetic field and phase drviations on the heat transfer in the cavity. In fact, it is endeavored to express the best situation for heat transfer and fluid flow with the considered parameters. Hence, the Al_2O_3–water nanofluid on laminar natural convection heat transfer at the presence of a magnetic field in sinusoidal temperature distribution on vertical side walls of the cavity by LBM was investigated.

2. Mathematical formulation

2.1 Problem statement

A two-dimensional square cavity is considered for the present study with the physical dimensions as shown in the **Fig. 1.** The side walls of the cavity have spatially varying sinusoidal temperature distributions. The horizontal walls are adiabatic. The cavity is filled with water and Al_2O_3 nanoparticles. The nanofluid is Newtonian and incompressible. The flow is considered to be steady, two dimensional and laminar, and the radiation effects are negligible. The thermo-physical properties of the base fluid and the nanoparticles are given in **Table 1**.

Table 1. Thermo-physical properties of water and nanoparticles

	ρ (kg /m³)	C_p (J/kg K)	K (W/mK)	β (K^{-1})
Pure water	997.1	4179	0.613	21×10^{-5}
Al_2O_3	**3970**	**765**	**40**	**0.85×10^{-5}**

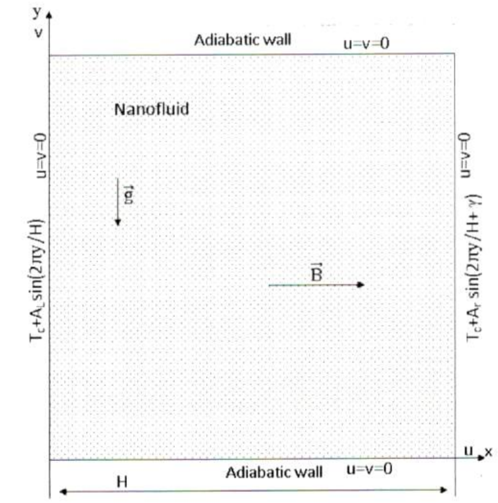

Fig.1 Geometry of the present study with boundary conditions

The density variation in the nanofluid is approximated by the standard Boussinesq model. The magnetic field strength B_0 is applied at an angle γ with respect to the coordinate system. It is assumed that the induced magnetic field produced by the motion of an electrically conducting fluid is negligible compared to the applied magnetic field. Furthermore, it is assumed that the viscous dissipation and Joule heating are neglected.
Therefore, governing equations can be written in dimensional form as follows:

$$\frac{\partial u}{\partial x}+\frac{\partial v}{\partial y}=0 \tag{1}$$

$$\rho_{nf}(u\frac{\partial u}{\partial x}+v\frac{\partial u}{\partial y})=-\frac{\partial p}{\partial x}+\mu_{nf}(\frac{\partial^2 u}{\partial x^2}+\frac{\partial^2 u}{\partial y^2}) \tag{2}$$

$$\rho_{nf}(u\frac{\partial v}{\partial x}+v\frac{\partial v}{\partial y})=-\frac{\partial p}{\partial y}+\mu_{nf}(\frac{\partial^2 v}{\partial x^2}+\frac{\partial^2 v}{\partial y^2})+F_y \tag{3}$$

$$u\frac{\partial T}{\partial x}+v\frac{\partial T}{\partial y}=\alpha_{nf}(\frac{\partial^2 T}{\partial x^2}+\frac{\partial^2 T}{\partial y^2}) \tag{4}$$

$$F_y=-\frac{Ha^2\mu_{nf}}{H^2}v+(\rho\beta)_{nf}g(T-T_m) \tag{5}$$

$$Ha=HB_0\sqrt{\frac{\sigma_{nf}}{\mu_{nf}}} \tag{6}$$

The classical models reported in the literature are used to determine the properties of the nanofluid:

$$\rho_{nf}=(1-\phi)\rho_f+\phi\rho_p \tag{7}$$

$$(\rho c_p)_{nf}=(1-\phi)(\rho c_p)_f+\phi(\rho c_p)_p \tag{8}$$

$$(\rho\beta)_{nf}=(1-\phi)(\rho\beta)_f+\phi(\rho\beta)_p \tag{9}$$

$$\alpha_{nf}=\frac{k_{nf}}{(\rho c_p)_{nf}} \tag{10}$$

In the above equations, ϕ is the solid volume fraction, ρ is the density, σ is the electrical conductivity, α is the thermal diffusivity, c_p is the specific heat at constant pressure and β is the thermal expansion coefficient of the nanofluid, γ is the direction of the magnetic field. The effective dynamic viscosity and thermal conductivity of the nanofluid can be modelled by:

$$\mu_{nf}=\frac{\mu_f}{(1-\phi)^{2.5}} \tag{11}$$

$$k_{nf}=k_f\frac{k_p+2k_f-2\phi(k_f-k_p)}{k_p+2k_f+\phi(k_f-k_p)} \tag{12}$$

The governing equations are subject to the following boundary conditions:

Bottom wall $\quad u=v=0 \quad \left.\frac{\partial T}{\partial y}\right|_{y=0}=0$

Top wall $\quad u=v=0 \quad \left.\frac{\partial T}{\partial y}\right|_{y=H}=0$ (13)

Left wall $\quad u=v=0 \quad T(0,y)=T_C+A_l\sin(2\pi y/H)$

Right wall $\quad u=v=0 \quad T(H,y)=T_C+A_r\sin(2\pi\frac{y}{H}+\gamma)$

2.2 Lattice Boltzmann Method

For the incompressible non isothermal problems, Lattice Boltzmann Method (LBM) utilizes two distribution functions, f and g, for the flow and temperature fields respectively.
For the flow field:

$$f_i(\mathbf{x}+\mathbf{c}_i\Delta t, t+\Delta t) = f_i(\mathbf{x},t) - \frac{1}{\tau_v}\left(f_i(\mathbf{x},t) - f_i^{eq}(\mathbf{x},t)\right) + \Delta t F_i \quad (14)$$

For the temperature field:

$$g_i(\mathbf{x}+\mathbf{c}_i\Delta t, t+\Delta t) = g_i(\mathbf{x},t) - \frac{1}{\tau_\alpha}\left(g_i(\mathbf{x},t) - g_i^{eq}(\mathbf{x},t)\right) \quad (15)$$

Where the discrete particle velocity vectors defined by $\mathbf{c}_i$, Δt denotes lattice time step which is set to unity. τ_v, τ_α are the relaxation time for the flow and temperature fields, respectively. f_i^{eq}, g_i^{eq} are the local equilibrium distribution functions that have an appropriately prescribed functional dependence on the local hydrodynamic properties which are calculated with Eqs.(16) and (17) for flow and temperature fields respectively.

$$f_i^{eq} = \omega_i\rho\left[1 + \frac{3(\mathbf{c}_i.\mathbf{u})}{c^2} + \frac{9(\mathbf{c}_i.\mathbf{u})^2}{2c^4} - \frac{3\mathbf{u}^2}{2c^2}\right] \quad (16)$$

$$g_i^{eq} = \omega_i' T\left[1 + 3\frac{\mathbf{c}_i.\mathbf{u}}{c^2}\right] \quad (17)$$

$\mathbf{u}$ and ρ are the macroscopic velocity and density, respectively. c is the lattice speed which is equal to $\Delta x/\Delta t$ where Δx is the lattice space similar to the lattice time step Δt which is equal to unity, ω_i is the weighting factor for flow, ω_i' is the weighting factor for temperature. D2Q9 model for flow and D2Q4 model for temperature are used in this work so that the weighting factors and the discrete particle velocity vectors are different for these two models and they are calculated with Eqs (18-20) as follows:

For D2Q9

$$\omega_0 = \frac{4}{9}, \omega_i = \frac{1}{9} \text{ for } i=1,2,3,4 \text{ and } \omega_i = \frac{1}{36} \text{ for } i=5,6,7,8 \quad (18)$$

$$\mathbf{c}_i = \begin{cases} 0 & i=0 \\ (\cos[(i-1)\pi/2], \sin[(i-1)\pi/2])c & i=1,2,3,4 \\ \sqrt{2}(\cos[(i-5)\pi/2+\pi/4], \sin[(i-5)\pi/2+\pi/4])c & i=5,6,7,8 \end{cases} \quad (19)$$

For D2Q4

The temperature weighting factor for each direction is equal to $\omega_i' = 1/4$.

$$\mathbf{c}_i = (\cos\cos[(i-1)\pi/2], \sin[(i-1)\pi/2])c \quad (20)$$
$$i = 1,2,3,4$$

The kinematic viscosity v and the thermal diffusivity α are then related to the relaxation time by Eq. (21):

$$v = \left[\tau_v - \frac{1}{2}\right]c_s^2\Delta t \qquad \alpha = \left[\tau_\alpha - \frac{1}{2}\right]c_s^2\Delta t \quad (21)$$

Where c_s is the lattice speed of sound witch is equals to $c_s = c/\sqrt{3}$. In the simulation of natural convection, the external force term F appearing in Eq. (14) is given by Eq.(22)

$$F_i = \frac{\omega_i}{c_s^2} F.c_i \quad (22)$$

Where $F = F_y$

The macroscopic quantities, $\mathbf{u}$ and T can be calculated by the mentioned variables, with Eq.(23-25).

$$\rho = \sum_i f_i \quad (23)$$

$$\rho\mathbf{u} = \sum_i f_i\mathbf{c}_i \quad (24)$$

$$T = \sum_i g_i \quad (25)$$

2.3 Non-dimensional parameters

By fixing Rayleigh number, Prandtl number and Mach number, the viscosity and thermal diffusivity are calculated from the definition of these non dimensional parameters. $v_f = N.Ma.c_s\sqrt{\Pr/Ra}$ Where N is number of lattices in y-direction. Rayleigh and Prandtl numbers are defined as $Ra = g\beta_f H^3(T_h - T_c)/v_f\alpha_f$ and $\Pr = v_f/\alpha_f$, respectively. Mach number should be less than $Ma = 0.3$ to insure an incompressible flow. Therefore, in the present study, Mach number was fixed at $Ma = 0.1$. Nusselt number is one of the most important dimensionless parameters in the description of the convective heat transport. Nusselt number is one of the most important dimensionless parameters in the description of the convective heat transport. The local Nusselt number and the average value at the bottom and the right walls are calculated as:

$$\text{Nul} = -\frac{k_{nf}}{k_f}\frac{H}{T_h - T_c}\left.\frac{\partial T}{\partial x}\right|_{x=0}$$
$$\text{Nur} = -\frac{k_{nf}}{k_f}\frac{H}{T_h - T_c}\left.\frac{\partial T}{\partial x}\right|_{x=H} \quad (26)$$

$$\text{Nu} = \frac{1}{H}\int_{heating\ half} \text{Nur}\,dy + \frac{1}{H}\int_{heating\ half} \text{Nul}\,dy \quad (27)$$

$$\text{Nu}^*(\phi) = \frac{\text{Nu}(\phi)}{\text{Nu}(\phi=0)} \quad (28)$$

3. Results and discussion

3.1 Validation of the numerical code

Lattice Boltzmann Method scheme was utilized to obtain the numerical simulations in a cavity with a sinusoidal boundary condition that is filled with nanofluid of water/Al_2O_3. **Fig. 2** demonstrates the effect of grid resolution and the lattice sizes (20x20), (40x40), (60x60), (80x80) and (100x100) for Ha=0 and $\phi = 0$ by calculating the average Nusselt number for Ra=10^3 and 10^5, it was found that a grid size of (100x100) ensures a grid independent solution. In order to check on the accuracy of the numerical technique employed for the solution of the considered problem, the present numerical code was validated with the published study of Deng et al. [14] for the same cavity with sinusoidal boundary conditions for $\gamma = \pi/2$, Ra=10^5 and Pr=0.7. The results are presented in

Fig.3 as streamlines and isotherms have a good agreement between both compared methods.

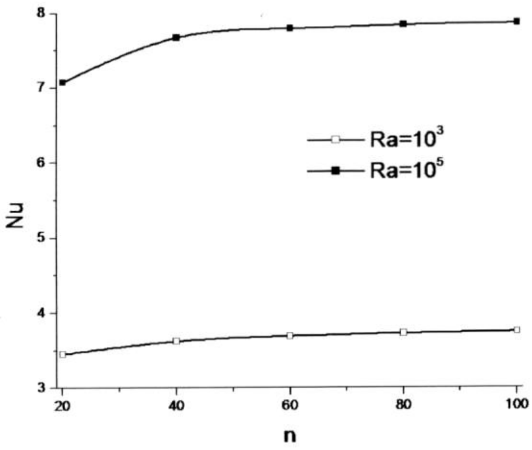

Fig. 2 Average Nusselt number for different uniform grids ($\phi = 0$, $\gamma=\pi/2$ and Ha=0)

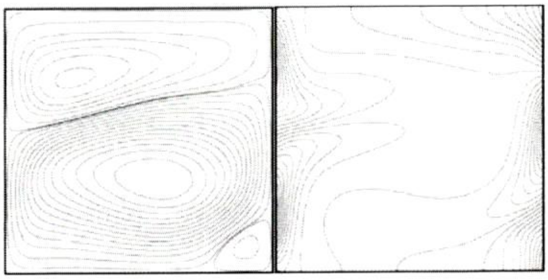

a

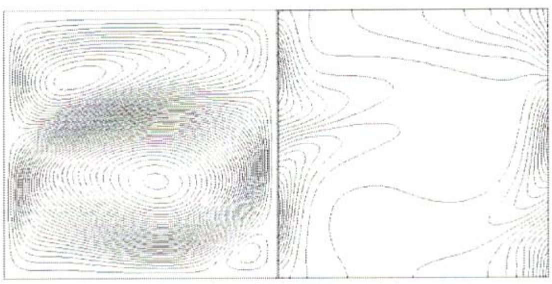

b

Fig. 3. Comparison of the streamlines and isotherms for Ra=10^5 and Pr = 0.7 between (a) numerical results by Deng et al. [14] and (b) the present result

3.2 Results and discussion

Fig.4 presents the effect of Hartmann number for different values of the Rayleigh number (Ra = 10^3, 10^4 and10^5) and for $\gamma = 0$ on the isotherms and streamlines of nanofluid (ϕ=0.04) and pure fluid (ϕ=0). For all Rayleigh number it demonstrates that the effect of nanoparticles on the isotherms decreases with the augmentation of Hartmann number. The thickness of the boundary layer decreases with the rise of Hartmann number and it results in decrease in heat transfer by the magnetic field, **Fig.5** shows the variation of average Nusselt number as function of Hartmann number for different Rayleigh number, the increase of Rayleigh number increases the heat transfer rate, on the contrary, the increase of the Hartmann decreases the heat transfer rate. The streamlines shows that the flow behavior is affected with the change in the Rayleigh number and the Hartmann number. the flow is characterized by four cells, The strength of these cells increases as the Rayleigh number increases and decreases as the Hartmann number increases. For all values of Rayleigh number, the application of the magnetic field has the tendency to slow down the movement of the fluid in the enclosure. The strength of these cells increases as the Rayleigh number increases and decreases as the Hartmann number increases. For all values of Rayleigh number, the application of the magnetic field has the tendency to slow down the movement of the fluid in the enclosure.

Fig.6 presents the variations of the local Nusselt numbers along the left sidewall and the right sidewall for various Hartmann numbers. At Ra=10^4 the heat transfer gets no remarkable change on both sidewalls even if the Hartmann number is increased but for Ra=10^5 it seems that the Nusselt number decreases while the Hartmann number is increased.

Fig.7 illustrate the variations of the local Nusselt numbers along the left sidewall and right sidewall at various Rayleigh numbers for Ha=10 and 50. For both walls, the curves drawn for the Nusselt numbers against y/H are approximately of sinusoidal shape like the thermal boundary. This indicates that the local heat transfer is directly affected by the temperature distribution on the surface. It is observed that the Rayleigh number effect is more significant for low Hartmann number.

Fig. 8 presents the effect of Hartmann number and solid volume fraction on the Nusselt number at Ra =5×10^4 and γ = 0. At small values of Hartmann number (Ha < 5), the addition of nanoparticles decreases the heat transfer, but if Hartmann number increases (5<Ha) the heat transfer increase as the solid volume fraction increases. The effect of nanoparticles is more significant for high Hartmann number.

Fig.9 indicate the local Nusselt number on the right and left sidewalls for various volume fractions at Ra=5×10^4, γ=0 and Ha=10 and 50. It is shown that the effect of nanoparticles is more significant for Ha = 50 which is consistent with **Fig.8**.

Fig.10 shows the effects of volume fractions and phase deviations for Ra =5×10^4 and for various Hartmann numbers on the average Nusselt number and the dimensionless average Nusselt number. For all Hartmann number and phase deviations the heat transfer increases with the rise of volume fraction. For Ha=20 heat transfer increases with the rise of phase deviations, the most heat transfer was obtained for $\gamma = \pi$. the best effect of nanoparticles is obtained in γ = 0. For Ha=50 heat transfer decreases from γ= 0 to $\pi/4$ and increases from $\gamma = \pi/2$ to π. The effect of nanoparticles decreases with the rise of phase deviation.

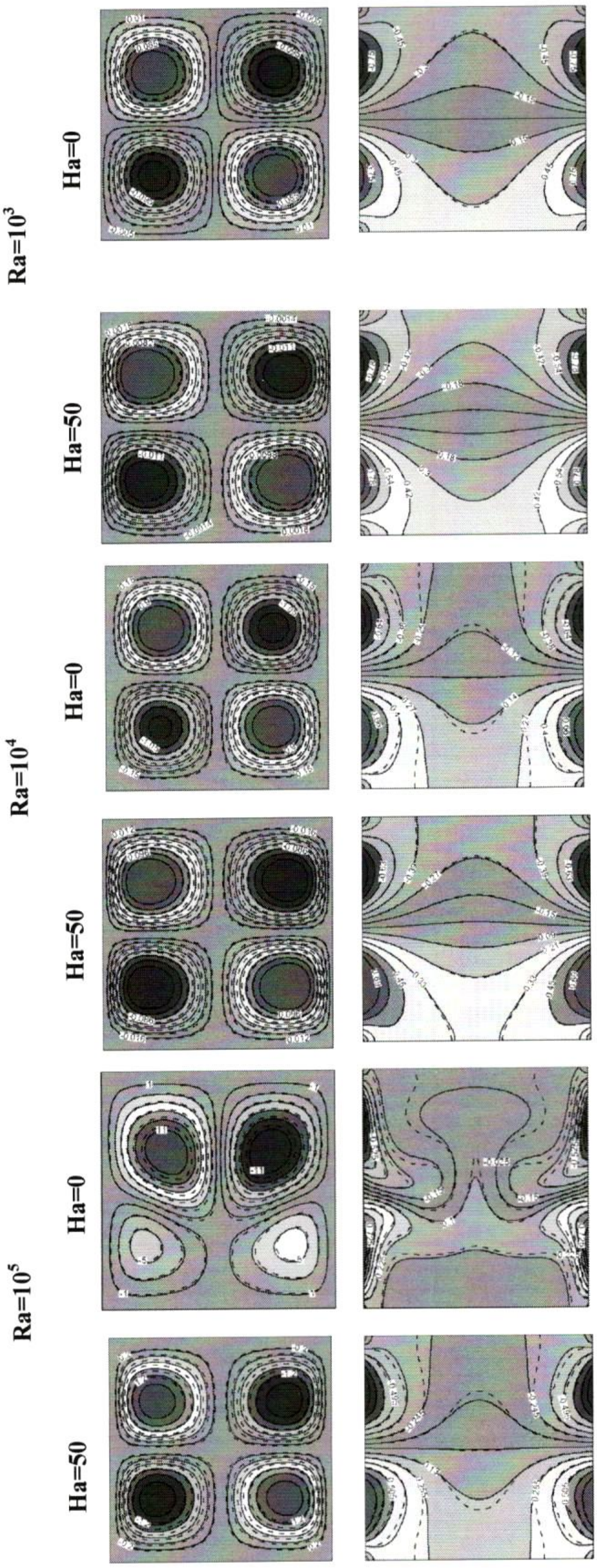

Fig. 4 Streamlines and isotherms for different Hartmann and Rayleigh numbers and for γ=0, (—) $\phi = 0.04$ and (- - -) $\phi = 0$

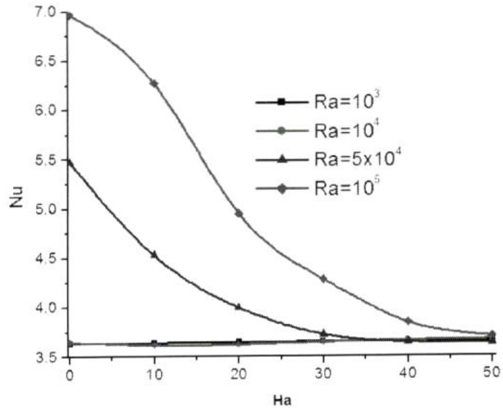

Fig. 5 Variation of the average Nusselt number with Hartmann number for different Rayleigh number for γ=0 and $\phi = 0$

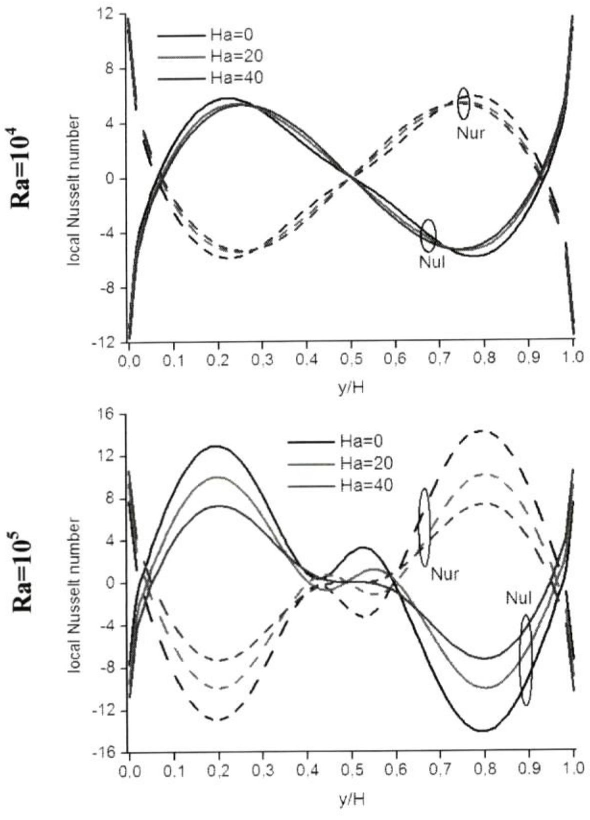

Fig. 6 Variation of the local Nusselt number for different Hartmann number for Ra=10^4 and Ra=10^5 for γ=0 and $\phi = 0$

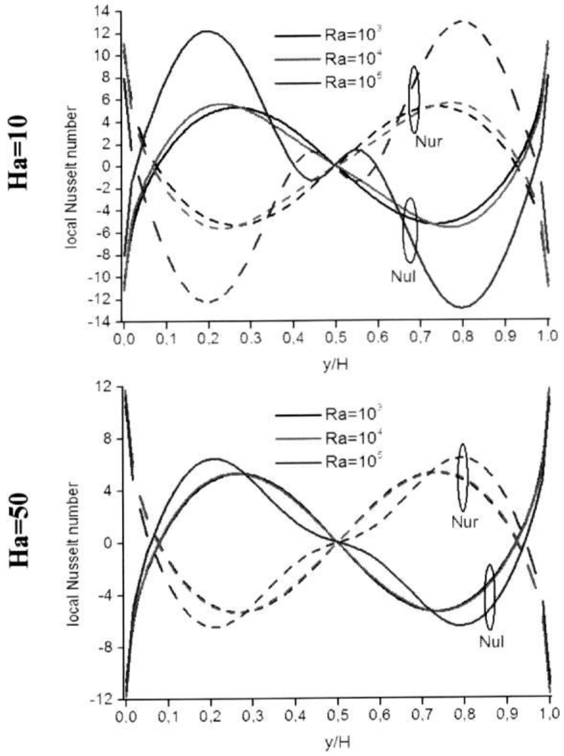

Fig. 7 Variation of the local Nusselt number for different Rayleigh number for Ha=10 and Ha=50 for γ=0 and $\phi = 0$

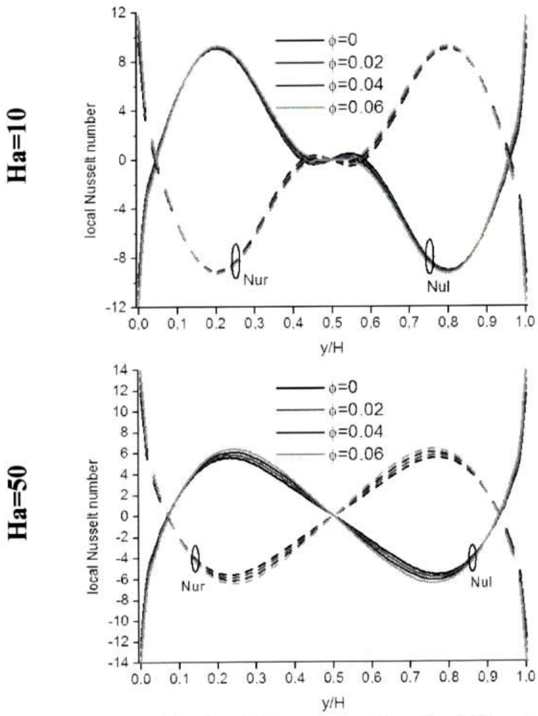

Fig. 9. Variation of the local Nusselt number for different solid volume fraction at γ=0, Ra=5x10^4 for Ha=0 and Ha=50

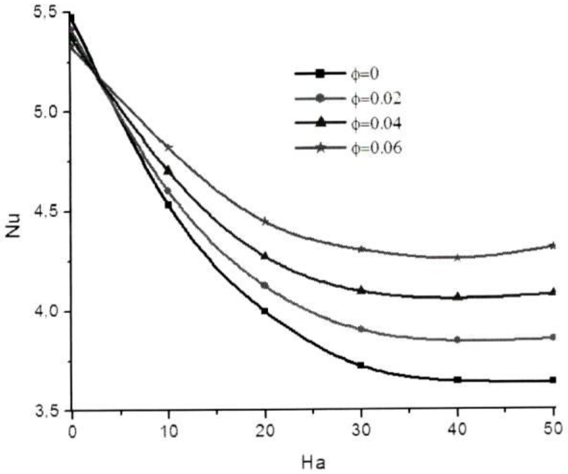

Fig. 8 Variation of the average Nusselt number with Hartmann number for different volume fraction for Ra=5x10^4 γ=0 and $\phi = 0$

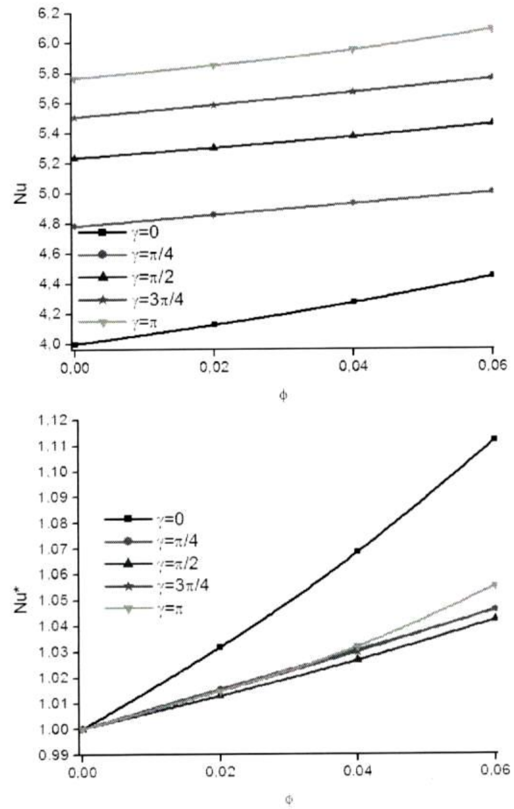

a

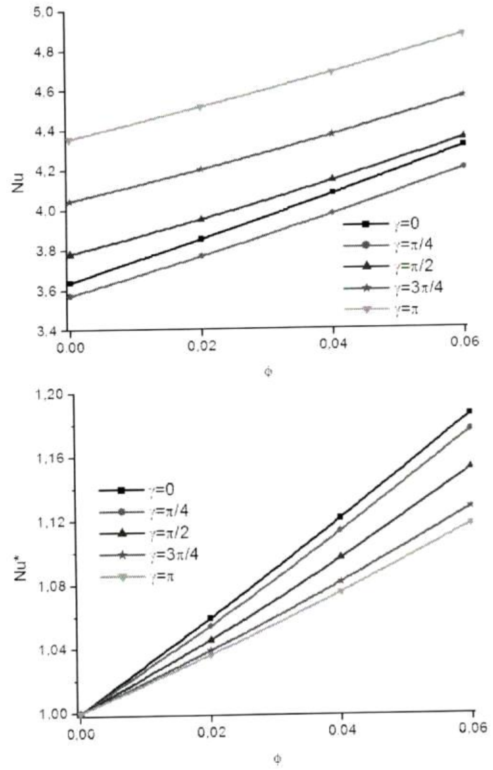

b

Fig.10. Variation of the average Nusselt number and dimensionless average Nusselt number as function of solid volume fraction for different phase deviations for Ra=5x10^4, Ha=20 (a) and Ha=50 (b)

4. Conclusions

In this paper the effects of a magnetic field on nanofluid flow in a cavity with a sinusoidal boundary condition has been analyzed with Lattice Boltzmann Method. This study has been carried out for the pertinent parameters in the following ranges: the Rayleigh number of base fluid, Ra=10^3–10^5, Hartmann number of the magnetic field between 0 and 90, the volume fraction is from ϕ=0 to 0.06 and the the phase deviation (γ=0, π/4, π/2, 3π/4 and π). The results show that the heat transfer rate increases with an increase of the Rayleigh number but it decreases with an increase of the Hartmann number. Also it is observed that the Phase deviation control the heat transfer rate.

Nomenclature

B	Magnetic field (Tesla)
c	Lattice speed (ms^{-1})
c_s	Speed of sound (ms^{-1})
$\mathbf{c_i}$	Discrete particle speeds (ms^{-1})
F	External forces (kg m s^{-2})
f	Density distribution functions (kgm^{-3})
f^{eq}	Equilibrium density distribution functions (kgm^{-3})
g	Internal energy distribution functions (K)
g^{eq}	Equilibrium internal energy distribution (K)
$\vec{g}$	Gravity vector (m s^{-2})

References

1. S. Ostrach, Natural convection in enclosures, *Journal of Heat Transfer*, vol 110, pp. 1175-1190, 1988.
2. M. Moreau, Magnetohydrodynamics, Kluwer Acadamic Publishers, The Netherlands, 1990.
3. H. Ozoe, K. Okada, The effect of the direction of the external magnetic field on the three dimensional natural convection in a cubical enclosure, *International Journal of Heat and Mass Transfer*, vol. 32, pp. 1939-1954, 1989
4. Y. Al-Badawi and H. M. Duwairi . MHD Natural Convection in Iso-Flux Enclosures Filled With Porous Medium. *Int. J. Heat Technol.* Vol. 28 (2), pp. 87-91, 2010.
5. S. Abishek and S. S. Katte. Magnetohydrodynamic thermo-solutal buoyant darcy convection in a square enclosure. *Int. J. Heat Technol*, vol. 28(2), pp. 105-116, 2010.
6. N. Ahmed and D. Kalita, MHD oscillatory free convective flow past a vertical plate in slip-flow regime with variable suction and periodic plate temperature, *Int. J. Heat Technol*, vol. 28(1), pp. 141-147, 2010.
7. F.G. Shehadeh and H. M. Duwairi, MHD natural convection with joule and viscous heating effect in porous media-filled enclosures, *Int. J. Heat Technol*, vol. 28(1), pp. 31-36, 2010.
8. F. Lai, Y. Yang, Lattice Boltzmann simulation of natural convection heat transfer of Al_2O_3/water nanofluids in a square enclosure, *International Journal of Thermal Sciences*, vol. 50, pp. 1930-1941, 2011.
9. A.H. Mahmoudi, M. Shahi, A.M. Shahedin, N. Hemati, Numerical modeling of natural convection in an open cavity with two vertical thin heat sources subjected to a nanofluid, *International Communications in Heat and Mass Transfer*, vol.38, pp.110-118,2011.
10. H. Nemati, M. Farhadi, K. Sedighi , M.M. Pirouz, E. Fattahi, Numerical simulation of fluid flow around two rotating side by side circular cylinders by Lattice Boltzmann method, *International Journal of Computational Fluid Dynamics* vol. 24, pp. 83–94, 2010.
11. M. Mehravaran, S.K. Hannani, Simulation of buoyant bubble motion in viscous flows employing lattice Boltzmann and level set methods, *Scientia Iranica*, vol. 18, pp. 231–240, 2011
12. D. Martinez, S. Chen, W.H. Matthaeus, Lattice Boltzmann magneto hydrodynamics, *Physics of Plasmas*, vol. 1, pp. 1850–1867, 1994
13. H. Nemati, M. Farhadi, K. Sedighi, E. Fattahi, A.A.R. Darzi, Lattice Boltzmann simulation of nanofluid in lid-driven cavity, *International Communications in Heat and Mass Transfer*, vol. 37, pp.1528–1534, 2010.
14. Q.H. Deng, J. Chang, Natural convection in a rectangular enclosure with sinusoidal temperature distributions on both sidewalls, *Numer. Heat Transfer A*, vol. 54, pp.507–524, 2008